

Effect of Hard Materials Nanocoating on Fins in (Thermosyphon) HPHE with Nano Working Fluid

Aysar A. Alamery*, Hussein A. Jawad*, Hani Aziz Ameen**, Zainab F. Mahdi*

*Institute of laser for postgraduate studies, University of Baghdad, Iraq.

** Dies and Tools Engineering Department, Technical Collage, Baghdad, Iraq.

Abstract - Introducing nanocoating of fins to improve the heat transfer characteristics is a novel approach. Modeling of the nanocoating on fins in Thermosyphon heat exchangers using ANSYS software is presented. The temperature distribution and thermal resistance were investigated. Five nanocoating materials (BN, WC, HFB₂, MgO and MOSi₂) are used. The maximum enhancement occurred at the evaporator section of 63.58 for BN, 38.37 for WC, 41.92 for HFB₂, 44.50 for MgO and 50.62 for MOSi₂. Results show the best group is the nitrides group which gave an important indication that using the nanocoating just in the evaporator section to reduce the cost. The large amount of heat transfer occurs in the evaporator section according to the result of thermal resistance so a large benefit of latent heat of the air is guiding to increase the energy saving when using HPHE in HVAC systems.

Keywords: HVAC, (Thermosyphon) HPHE, ANSYS, Nanocoat, temperature distribution, Thermal resistance.

1. INTRODUCTION

Energy saving is one of the main subjects in industry especially in HVAC systems. Air conditioning is amongst the most energy consuming systems which need more attention regarding reduction of energy consumption. Heat pipe heat exchangers (HPHX) are proposed as a solution to energy consuming problem [1]. Heat pipes are heat transfer devices which use the principles of thermal conduction and latent heat of vaporization to transfer heat effectively at very fast rates [2]. It is essentially a passive heat transfer device with an extremely high effective thermal conductivity [3] and very efficient for the transport of heat with a small temperature difference via the phase change of the working fluid [4]. The two-phase heat transfer mechanism results in heat transfer capabilities from one hundred to several thousand times that of an equivalent piece of copper [3]. There are two types of heat pipes depending on how the condensed working fluid is returned to the evaporator section, namely gravity assisted heat pipes and heat pipes with wicks. In gravity assisted heat pipes the condensed fluid is returned due to gravitational forces whereas in heat pipes with wicks the condensed fluid is returned due to the capillary action through wicks. The use of heat pipes in heat exchangers results in many advantages such as compactness, low weight, high heat recovery effectiveness, no moving parts, pressure tightness, complete separation of hot and cold fluids and high reliability [2] relative economy, no external power

requirements, reduce primary energy consumption, thus reducing air pollutions. In HVACs an important role of the HPHX and is to recover heat from warm outdoor air reheat the dew-point air stream and as a result save energy of reheating [1]. Key factors affecting on thermal performance of a HPHE are: velocity, relative humidity (RH) and dry-bulb temperature (DBT) of input air, type and filling ratio (FR). Heat pipe technology has found increasing applications in enhancing the thermal performance of heat exchangers in microelectronics, energy saving in HVACs [5]. Also for operating rooms, surgery centers, hotels, cleanrooms etc., temperature regulation systems for the human body and other industrial sectors and are passive components used to improve dehumidification by commercial forced-air HVAC systems. They are installed with one end upstream of the evaporator coil to pre-cool supply air and one downstream to re-heat supply air. This allows the system's cooling coil to operate at a lower temperature, increasing the system latent cooling capability. Heat rejected by the downstream coil reheats the supply air, eliminating the need for a dedicated reheat coil. Heat pipes can increase latent cooling by 25-50% depending upon the application.

Conversely, since the reheat function increases the supply air temperature relative to a conventional system, a heat pipe will typically reduce sensible capacity [6]. **H.A. Mohammed et al. (2013)** [7] studied numerically the effect of using louvered strip inserts placed in a circular double pipe heat exchanger on the thermal and flow fields utilizing various types of nanofluids. **S. Ravitej Rajuet et al. (2013)** [2] presented numerical simulation of an air to air Gravity Assisted Heat Pipe Heat Exchanger (GAHPHE) which uses methanol as a working fluid based on effectiveness number of transfer units method.

Symbols

HVACs = Heating, Ventilation and Air conditioning systems.

K = Thermal Conductivity ($W.m^{-1}K^{-1}$)

C_p = Specific Heat ($J.kg^{-1}K^{-1}$)

ρ = Density ($kg.m^{-3}$)

T_e = Evaporator Temperature (K)

T_a = Adiabatic Section Temperature (K)

T_c = Condenser Temperature (K)

T = Absolute temperature

T_o = Ambient temperature

ϵ = Emissivity of the surface
 h = Convection coefficient.
 \bar{T}_i = Internal fluid control volume temperature
 \bar{T}_h, \bar{T}_c = The average hot stream and cold stream control volume temperatures
 \dot{m} = mass flow rate of the air into the evaporator or condenser section, $\text{kg}\cdot\text{s}^{-1}$
 \dot{Q} = heat, W
 R = Thermal resistance, $K\cdot W^{-1}$
 HP= heat pipe
 HE=heat exchanger

$$A = \text{Area}, m^2$$

L=length, m
 d = diameter, m
 K=keypoint
 Cyl4=Draw cylinder
 OTR=Outer tube radius
 ITR=Inter tube radius

Subscript

c = Condenser, cold
 e = evaporator, exit
 h =hot
 w = wall of the heat pipe
 i = Inside
 o = outside

2. MODELING OF HEAT PIPE HEAT EXCHANGER

Heat pipe is a device which operates in a closed loop two phase (vapor-liquid) thermodynamic cycle to transfer heat at high rates from one point to another with a very small change in temperature along the pipe. The heat pipe in its simplest configuration is a closed, generally built of circular tubes and evacuated cylindrical vessel [3]. It consists of an evacuated-closed tube filled with certain amount of a suitable pure working fluid [4]. During operation, heat is added through the bottom section (evaporator) and the working fluid becomes vapor. The vapor travels through the middle section (adiabatic section) to the top section (condenser) of the tube. In the condenser, the vapor releases the latent heat to the condenser wall and becomes liquid in contrast to a heat pipe, which utilizes capillary forces for liquid return; the Thermosyphon relies on gravitational or centrifugal force to return the condensed liquid to the evaporator [8]. The simulation of the heat pipe is achieved from the real design [9] as shown in Fig. (1), in which heat pipe is divided into three main sections, evaporator, condenser and adiabatic.

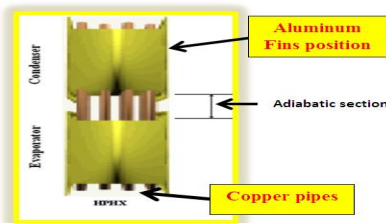


Fig. (1) Real design of the heat pipe

The dimensions of the model for the heat pipe were constructed in ANSYS _Preprocessor package. The height of the modeled heat pipe is 945 mm while its outer diameter is 15.875 mm. The evaporator and condenser sections have a height of 305 mm as shown in Fig. (2).

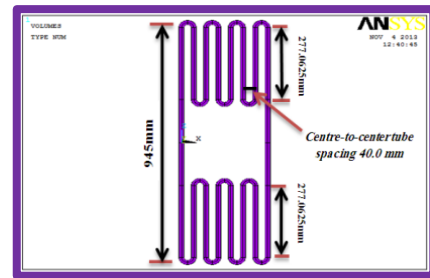


Fig. (2) The dimensions of the tube used in the analysis

The pipe wall attached to the 262 fins with dimensions shown in Fig. (3).

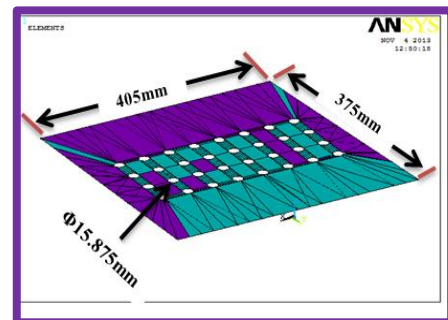


Fig. (3) Dimensions of the fin

The assembly system of the heat pipe (tubes and fins) can be shown in Fig. (4).

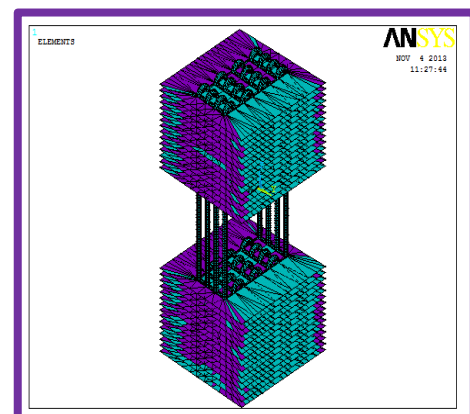


Fig. (4) Heat pipe model

Once the geometry was constructed, the mesh generation process was then carried by define three types of elements that are used in building the model (plane55, solid70, shell131). Dragging process was used to construct the heat pipe with properties ($K=398 \text{ W}\cdot\text{m}^{-1}\text{K}^{-1}$, $C_p=384 \text{ J}\cdot\text{kg}^{-1}\text{K}^{-1}$, $\rho=8954 \text{ kg}\cdot\text{m}^{-3}$) [10]. Firstly the pipe section is drawn and meshed with (plane 55) [11] as shown in Fig. (5)

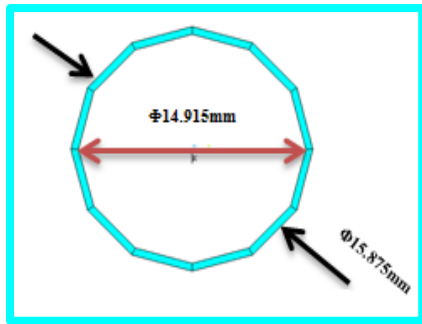


Fig. (5) section of heat pipe

Then it's dragged along the height of the heat pipe (945mm) with (solid70) [11] as shown in Fig. (6)

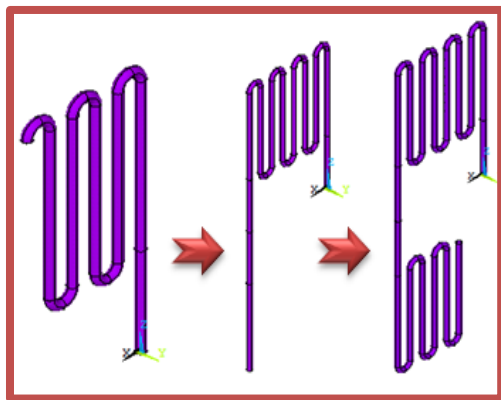
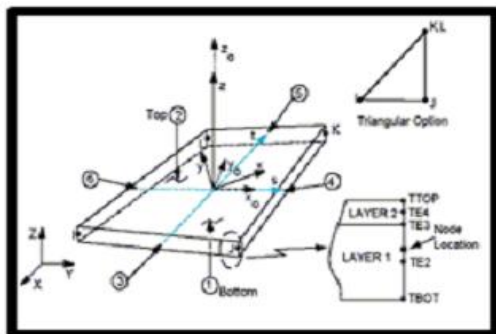
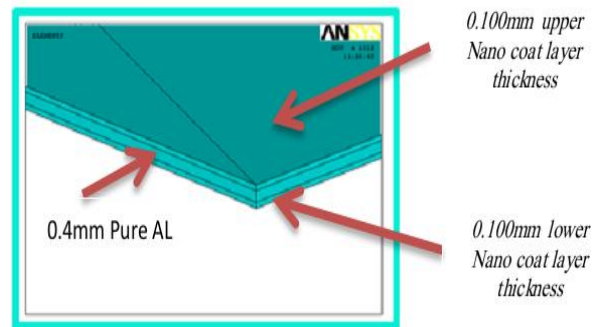


Fig. (6)dragging process

After that, fin made of Aluminum with thickness of 0.4mm and properties ($K= 237 \text{ W.m}^{-1}\text{K}^{-1}$, $C_p=905 \text{ J.kg}^{-1}\text{K}^{-1}$, $\rho=2707 \text{ kg.m}^{-3}$) [10]is modeled by direct generation using layer element (shell131) [11]. Fins with three layers are presented in the present work as in Fig. (7).



Shell131 element



Three layers

Fig. (7) Layers fin

The process is repeated to complete the (131 fins) in condenser and evaporator so the final stage is shown in

Fig. (8).

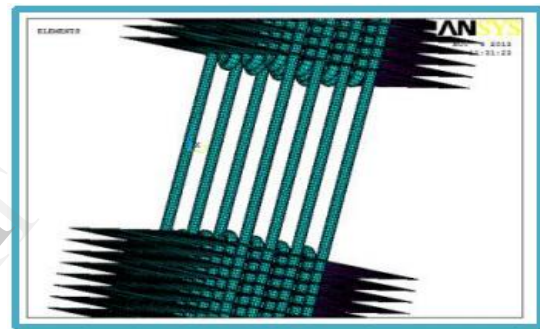


Fig. (8) Mesh of fins with tubes

The fin is modeled using of sectype and secdata commands and keyopt(3)=0 is used for transient analysis and keyopt(3)=1 is used for steady state analysis. The top and bottom layers are represented by the nanohard materials coating, five groups are used which are Nitrides, Carbides, Borides, Oxides and Silicide's (BN, WC, HFB₂, MgO and MOSi₂) respectively with their thermophysical properties [12]. Nanohard materials coating are particles that are usually less than 100nm in diameter .The particles are added with the aim of improving the thermal properties of the base metal (aluminum).

3. BOUNDARY CONDITIONS

The boundary conditions of the tube are used as shown in Fig. (9)[13], these results can be obtained by phase change properties from liquid (sliver water nanofluid) in evaporator section to the vapor in the condenser section.

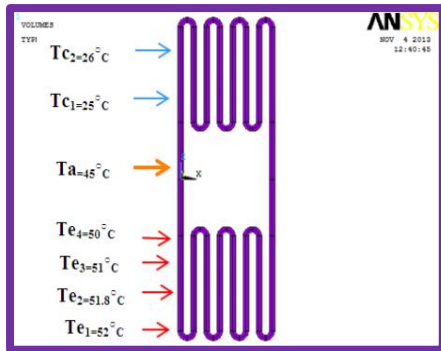


Fig. (9) Temperature distribution in the tube

Boundary conditions of the thermal model were specified as surface loads through ANSYS codes using element surf152 with convective and radiative heat losses to the ambient occurs across all free surfaces (evaporator and condenser) of the system. To consider convection and radiation on the fins surfaces, the heat loss is calculated by:

For radiation

$$q = \varepsilon\sigma(T^4 - T_o^4) \dots\dots (1)$$

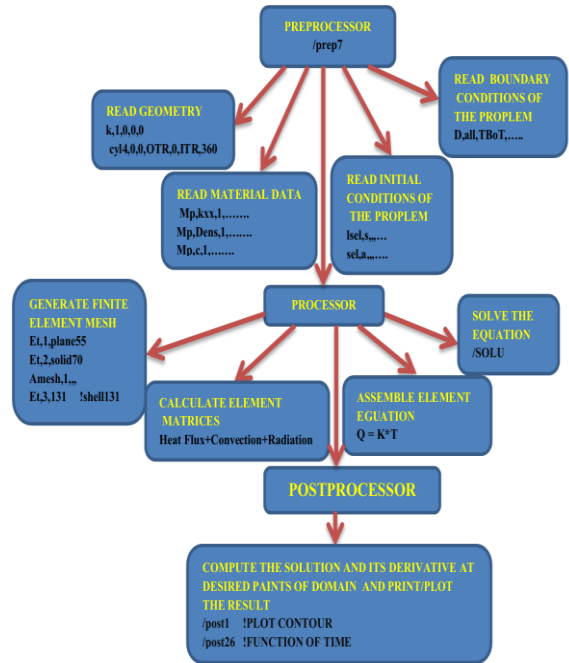
For convection

$$q = h(T - T_o) \dots\dots\dots (2)$$

Where T is absolute temperature of the fin, T_o is the ambient temperature, ε is the emissivity of the plate surface, $\sigma = 5.67 \times 10^{-8} \text{W.m}^{-2}\text{C}^{-4}$ and h is the convection coefficient. In the current model, when heat is applied to the evaporator end of the pipe making the working fluid vaporize, the working fluid can be transformed into vapor for temperature much less than the phase change which normally happens at atmospheric pressure. In the condenser section the latent heat of vaporization is removed from the flow by taking advantage of heat sink and hence condensation occurs. The following steps were built in APDL for convective and radiative boundary conditions

```

/sol
a,sel,s,loc
a,sel,a,loc
.
.
.
nsla,s,1
d,all,temp
nsl,s,node,,1e6
d,all,temp,
esel,s,ename,,surf152
sfe,all,conv,
allsel,all
    
```



4. HEAT PIPE'S THERMAL RESISTANCE

For a single two-phase closed Thermosyphon and for the thermal resistance diagram shown in Fig. (10),

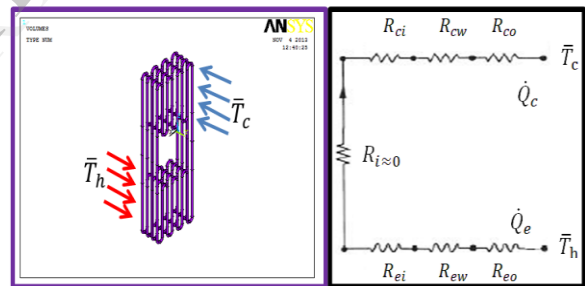


Fig. (10) Shows thermal resistance of heat pipe

heat is transferred from a heat source, through the evaporator wall, into the working fluid and then out through the condenser to the heat sink. This heat transfer rate may thus be conveniently expressed in terms of a temperature difference and the sum of a series of thermal resistances as [14]:

$$\dot{Q} = \frac{\bar{T}_h - \bar{T}_c}{\Sigma R} = \dot{Q}_e = \frac{\bar{T}_h - \bar{T}_i}{\Sigma R_e} = \dot{Q}_c = \frac{\bar{T}_i - \bar{T}_c}{\Sigma R_c} \dots\dots (3)$$

\bar{T}_i is the internal fluid control volume temperature

\bar{T}_h and \bar{T}_c are the average hot stream and cold stream control volume temperatures, and assuming a linear temperature distribution along each control volume, the average heating fluid and cooling fluid temperatures are given, respectively as :

$$\bar{T}_h = (T_{hi} + T_{ho})/2 \text{ and } \bar{T}_c = (T_{ci} + T_{co})/2$$

$$\sum R = R_e + R_c ,$$

$$\sum R_e = R_{eo} + R_{ew} + R_{ei}$$

and $\sum R_c = R_{ci} + R_{cw} + R_{co}$

$$R_{eo} = \frac{1}{h_{eo} A_{eo}}, R_{ew} = \frac{\ln\left(\frac{d_o}{d_i}\right)}{2\pi k L_e} \text{ and } R_{ei} = \frac{1}{h_{ei} A_{ei}}$$

$$R_{ci} = \frac{1}{h_{ci} A_{ci}}, R_{cw} = \frac{\ln\left(\frac{d_o}{d_i}\right)}{2\pi k L_c} \text{ and } R_{co} = \frac{1}{h_{co} A_{co}}$$

Where:

$$A_{eo} = \pi d_o L_e, A_{ei} = \pi d_i L_e$$

$$, A_{ci} = \pi d_i L_c \text{ and } A_{co} = \pi d_o L_c$$

Knowing the heating and cooling water inlet and outlet temperatures and the mass flow rates of the heating and cooling streams, the evaporator and condenser section heat transfer rates can be calculated in accordance with the conservation of energy as:

$$\dot{Q}_e = \dot{m}_e c_p (T_{hi} - T_{ho}) \pm \dot{Q}_{loss/gain} \dots(4)$$

$$\dot{Q}_c = \dot{m}_c c_p (T_{co} - T_{ci}) \pm \dot{Q}_{loss/gain} \dots(5)$$

The right hand terms $\dot{Q}_{loss/gain}$ in equations (4) and (5) account for the heat that is not transferred to the working fluid in the evaporator, and from the working fluid in the condenser, but that which is lost or gained from the environment through the heating/cooling jacket walls as well as through the structure supporting the Thermosyphon [14, 15]. For All tested fins, three fixed positions (1, 2 and 3) were taken in evaporator and condenser. Positions (2 and 3) were taken in the invers location according to the direction of air flow.

5. RESULTS AND DISCUSSION

As example of the results which approaches from the ANSYS program running after modeling the heat pipe as show in Fig (11)

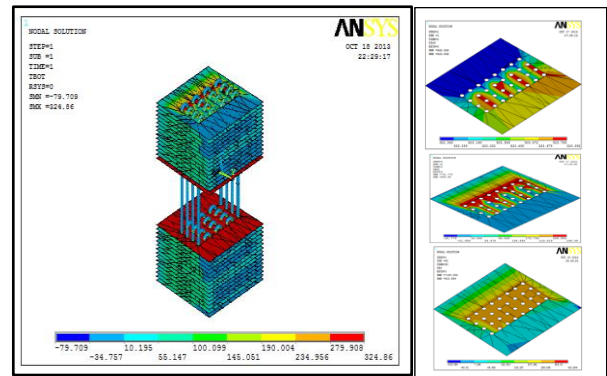


Fig. (11) Temperature distribution results from the ANSYS program for complete heat pipe heat exchanger and its fins alone

To investigate the influence of nanocoating on fins of heat pipe performance, all the thermal resistances were determined for the evaporator and condenser sections separately and the sum was considered as the total thermal resistance of the heat pipe. The respective average temperature of evaporator and condenser are recorded to calculate the system thermal resistance. Results in Fig (12) show the decrease of the thermal resistance along the evaporator section and it becomes zero in the adiabatic section after that a small increase occurs in the condenser section compared with the evaporator section this what made the large amount of heat transfer occur in the evaporator section.

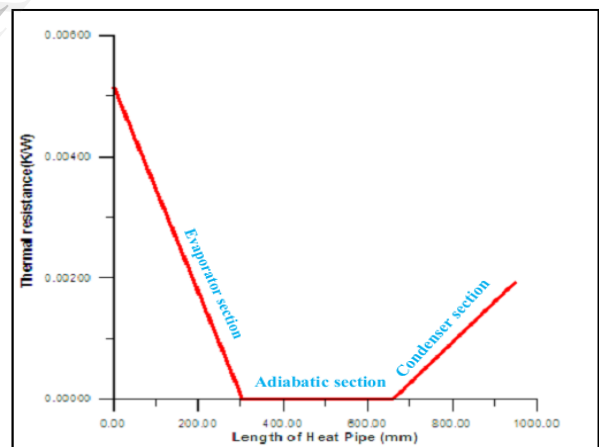


Fig. (12) Thermal resistance a long heat pipe

Fig. (13) Shows temperature distribution of two selected positions on fins (with and without nanocoat) in the evaporator and condenser section with the R_e and R_c . From these figures the results observed the large effect of nanocoat in the evaporator section especially when the HPHE operate in the transient conditions while the small and negative effect was observed in the condenser Section with the steady and transient operation conditions respectively.

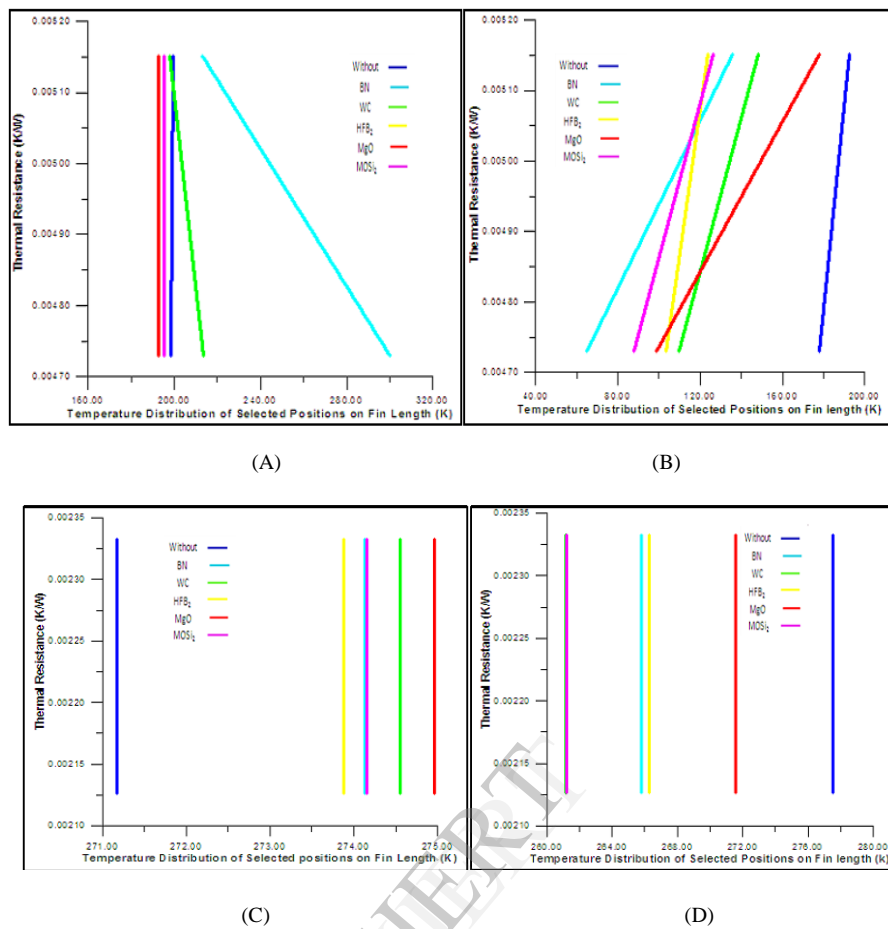


Fig.(13:A,B,C,D) Temperature distribution in two selected positions on fins (with and without nanocoat) in the evaporator and condenser sections with the R_e and R_c . A-Evaporator in steady state conditions. B- Evaporator in transient conditions. C-Condenser in steady state conditions. D-Condenser in transient conditions.

After calculations the percentages of thermal performance enhancement with nanocoating layers by using the equation $((Without\ Nanocoat - With\ Nanocoat) / (Without\ Nanocoat)) * 100$. The results were arranged in Table (1).As observed from the values the using of nanocoat were successful in the evaporator section especially in transient case of operation which is the fact.

Table (1): Percentages of thermal performance enhancement with nanocoating layers

Evaporator steady state					Evaporator Transient				
BN	WC	HFB ₂	MgO	MOSi ₂	BN	WC	HFB ₂	MgO	MOSi ₂
-51.03	-7.53	3.11	3.01	1.69	63.58	38.37	41.92	44.50	50.62
-7.15	0.77	3.43	3.33	1.99	29.80	22.96	35.71	7.82	34.43
Condenser steady state					Condenser Transient				
BN	WC	HFB ₂	MgO	MOSi ₂	BN	WC	HFB ₂	MgO	MOSi ₂
-1.09	-1.25	-1.00	-1.39	-1.10	4.21	5.89	4.05	2.14	5.86
-1.09	-1.25	-1.00	-1.39	-1.10	4.21	5.89	4.05	2.14	5.86

In the bottom of the evaporator section like fin 32(Fig. 14, A) difference was shown in the temperature distribution in three positions of fins. The fast response occurs in the Nitrides and Carbides groups in the position two. For the middle position like fin16(Fig. 14, B) of the evaporator section the same difference was shown approximately in the temperature distribution between the fins without nanocoat and the fins with five types of nanocoat in all positions in evaporator section in HPHE except the Carbides groups. In the top of the evaporator section like fin 4(Fig. 14, C) the effect was observed of nanocoat compared with the aluminum fins without nanocoat. All nanocoat groups show best and good results than the aluminum fins without nanocoat.

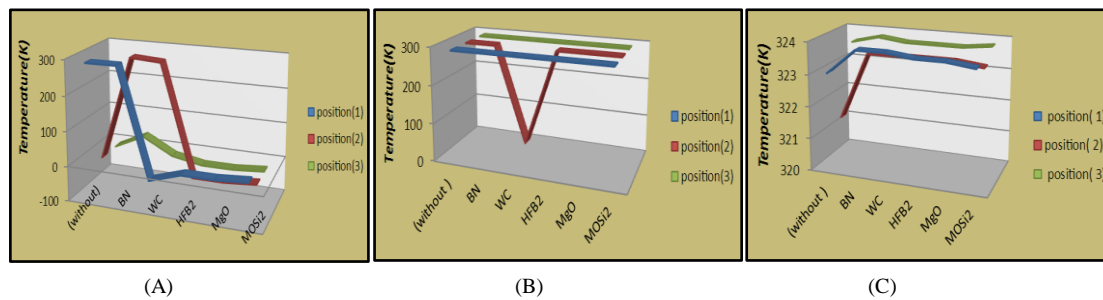


Fig (14) Temperatures distribution of evaporator in the case of steady state in three positions vertically and three position horizontally for each selected fins. A- Fin32, Evaporator, Steady State. B-Fin16,Evaporator, Steady State . C-Fin4, Evaporator, Steady State.

In the beginning of the condenser section like fin 3 (Fig. 15, A) there is no difference in the temperature distribution between the fins without nanocoat and fins with five types of nanocoat except the oxides group at position one where minimum temperature distribution occur .For the middle of the condenser section like fin 17 (Fig. 15, B) approximately the same difference was show in the temperature distribution between the fins without nanocoat and the fins with five types of nanocoat in all positions in this fin. The maximum temperature distribution occur at the Nitrides and oxides group while the minimum value at the Borides group .In the top of the condenser section like fin 31 (Fig. 15, C) the temperature distribution in fins with five types of nanocoat and fins without nanocoat are the same in the position two and three which represent the degree of air in this location equal 22°C .In position one the large difference in the temperature distribution between the fins without nanocoat and the fins with five types of nanocoat due to the near effect of nanofluid in all directions on the air stream.

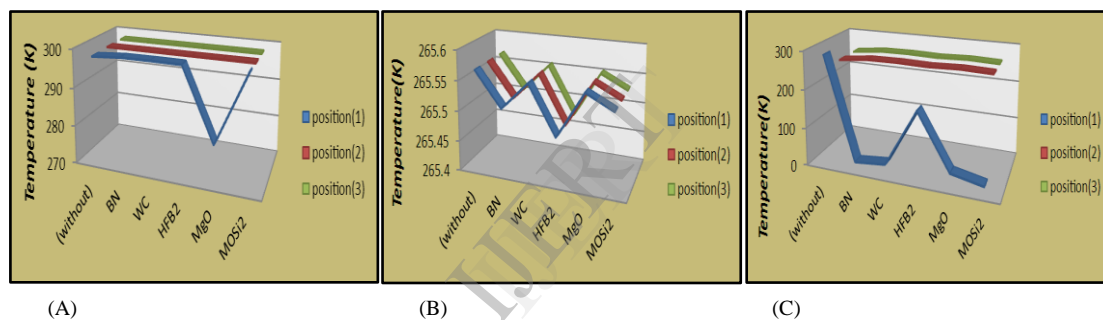


Fig (15) Temperatures distribution of condenser in the case of steady state in three positions vertically and three position horizontally for each selected fins. A- Fin3,Condenser,Steady State. B-Fin17,Condenser,Steady State. C-Fin31,Condenser,Steady State.

For transient condition, in the bottom of the evaporator like fin 32 (Fig. 16, A) a small difference is shown in the temperature distribution between fins without nanocoat and fins with five types of nanocoat especially at the fourth pipe of the evaporator section in HPHE .The maximum temperature distribution occur at the oxides group while the minimum value at the Boride group. The maximum temperature distribution occur in the middle of the evaporator section (Fig. 16, B) due to the effect of Nanofluid inside HPHE. In the middle of the Evaporator approximately the same difference was shown in the temperature was shown in the temperature distribution between the fins without nanocoat and the fins with five types of nanocoat in all positions in evaporator section in HPHE .The maximum temperature distribution occur at the Nitrides group while the minimum value at the oxide group .For the top of the same section (Fig. 16, C) the effect of nanocoat compared with the aluminum fins without nanocoat was shown. The best and low temperature occur at the Nitrides group which represents the cooling of air compared with its state in the inlet face of evaporator section.

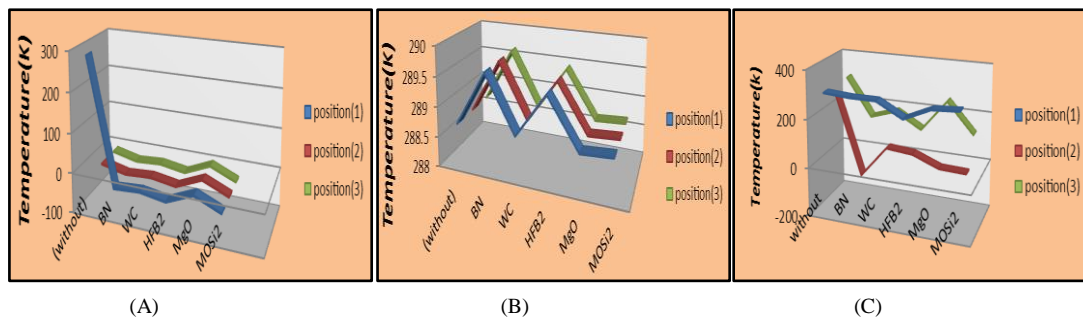


Fig (16) Temperatures distribution of evaporator in the case of transient in three positions vertically and three position horizontally for each selected fins. A- Fin32,Evaporator,Transient.B-Fin16,Evaporator,Transient .C-Fin4,Evaporator,Transient.

In the base of condenser (Fig. 17, A) a small difference was shown in the temperature distribution between the fins without nanocoat and the fins with five types of nanocoat especially at the fourth pipe of the condenser section in HPHE. The maximum temperature distribution occur at the oxides group while the minimum value at the Carbides group .The maximum temperature distribution occurs in the middle of the condenser section (Fig. 17, B) which due to the effect of Nano fluid insideHPHEwhile In the middle of the same section approximately the same difference in the temperature distribution between the finswithout nanocoat and the fins with five types of nanocoat in all positions in condenser section in HPHE was seen. The maximum temperature distribution occur atthe oxides groupwhile the minimum value at the Borides group .The maximum temperature distribution occur in the middle of the condenser section due to the effect of Nano fluid inside HPHE in this height . In the end of condenser (Fig. 17, C) figure shows the temperature distribution in fins with five types of nanocoat is smaller than fins without nanocoat especially at the middle of the condenser section in HPHE due to the effect of the nanofluid condensate completely .Coating the Aluminum fins plate with Nano material increase the heat dissipation from condenser compared with HPHE when using just nanofluid inside pipes without nanocoat.

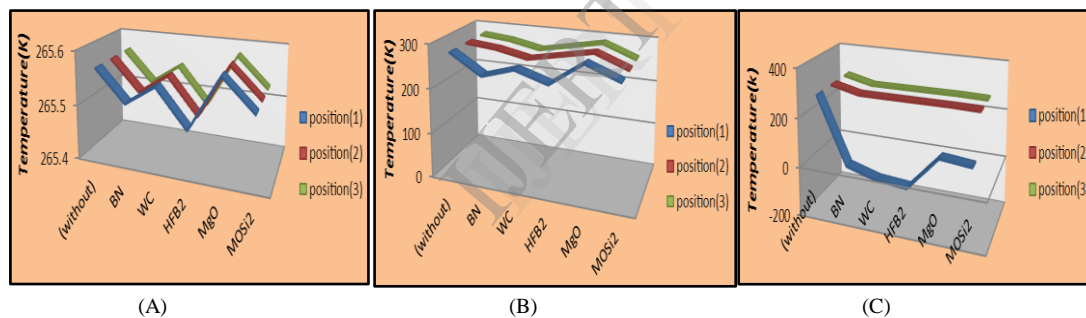


Fig (17) Temperatures distribution of condenser in the case of transient in three position vertically and three position horizontally for each selected fins. A-Fin3, Condenser, Transient .B-Fin17, Condenser, Transient.C-Fin31, Condenser, Transient.

6. CONCLUSIONS

One of the most advanced methods to improve the thermal conductivity of heat pipes is to coat the fins by Nano materials. It increases in effective surface area of heat flux absorbent and increases the effective thermal conductivity of the fluid. The effect of nanocoating on temperature distribution on the fins were explored in which the maximum enhancement occurred at the evaporator section with 63.58 for BN, 38.37 for WC, 41.92 for HFB₂, 44.50 for MgO and 50.62 for MOSi₂. This results show the best group of Nanohard materials for this purpose is the nitrides group .The calculations give important indication that using the nanocoat just in the evaporator section to reduce the cost. The large amount of heat transfer occur in the evaporator section according to the result of thermal resistance in this section then large benefit of latent heat of

the air this guide to increase the energy saving when using HPHE in HVAC systems .

REFERENCES

- [1] I.Abrishamchi, S. Mustafa Nowee , R. Rezazadeh and S.Hosseini Noie,"Effect Of Working Fluid On The Performance of Thermosyphon Heat Exchangers In Series Used In An Air ConditioningSystem",Proceedings of 2010 International Conferenceon Chemical Engineering and Applications (CCEA 2010),Singapore, pp.26-28 ,February 2010.
- [2] S. Ravitej Raju, M. Balasubramani, B. Nitin Krishnan,K. Kesavan and M. Suresh," Numerical Studies On The Performance Of Methanol Based Air To Air Heat Pipe Heat Exchanger", International Journal of ChemTech Research, Vol.5, No.2, pp. 925-934, April-June 2013.
- [3] A. Khare, A. Paul and G. Selokar," Design Development of Test-Rig to Evaluate performance of Heat Pipes in Cooling of Printed Circuit Boards", VSRD-MAP, Vol. 1 (2), pp. 65-79, 2011.
- [4] M. R. SARMASTI EMAMI, S. H. NOIE and M. KHOSHNOODI," Effect of Aspect Ratio and Filling Ratio on

- Thermal Performance of an Inclined Two-Phase Closed Thermosyphon", Iranian Journal of Science & Technology, Transaction B, Engineering, Printed in The Islamic Republic of Iran, Vol. 32, No. B1, pp. 39-51, 2008.
- [5] E. Firouzfard, M. Soltanieh, S. H. Noie and M. H. Saidi, "Investigation of heat pipe heat exchanger effectiveness and energy saving in air conditioning systems using silver nanofluid", Int. J. Environ. Sci. Technol. 9:587-594, 2012.
- [6] E. Firouzfard and M. Attaran, "A review of heat pipe heat exchangers activity in Asia", World Academy of Science, Engineering and Technology 47, 2008.
- [7] H.A. Mohammed, H.A. Hasan and M.A. Wahid, "Heat transfer enhancement of nanofluids in a double pipe heat exchanger with louvered strip inserts", International Communications in Heat and Mass Transfer 40, pp. 36-46, 2013.
- [8] P.G. Anjankar and R.B. Yarasu, "Experimental analysis of condenser length effect on the performance of thermosyphon", International Journal of Emerging Technology and Advanced Engineering, Volume 2, ISSN 2250-2459, March 2012.
- [9] Y.H. Yau, "Experimental thermal performance study of an inclined heat pipe heat exchanger operating in high humid tropical HVAC systems", International Journal of Refrigeration, 30, 1143-1152, 2007.
- [10] J.H. Lienhard IV and J.H. Lienhard V, "A heat transfer textbook", Third edition, 2001.
- [11] ANSYS, "ANSYS help", Release (1, 2011).
- [12] S. Zhang and N. Ali, "Nanocomposite thin films and coatings processing, properties and performance", Copyright by Imperial College Press, 2007.
- [13] S.H. Noie, S. Zeinali Heris, M. Kahani and S.M. Nowee, "Heat transfer enhancement using Al₂O₃/water nanofluid in a two-phase closed thermosyphon", International Journal of Heat and Fluid Flow, 30, 700-705, 2009.
- [14] R.T. Dobson and R. Laubscher, "Heat pipe heat exchanger for high temperature nuclear reactor technology", Frontiers in Heat Pipes (FHP), 4, 023002, 2013.
- [15] A. Meyer and R. T. Dobson, "A heat pipe heat recovery heat exchanger for a mini-drier", Journal of Energy in Southern Africa, Vol. 17, No 1, February 2006.

IJERT